This article was downloaded by:
On: *26 January 2011*
Access details: *Access Details: Free Access*
Publisher *Taylor & Francis*
Informa Ltd Registered in England and Wales Registered Number: 1072954 Registered office: Mortimer House, 37-41 Mortimer Street, London W1T 3JH, UK

Liquid Crystals

Publication details, including instructions for authors and subscription information:
http://www.informaworld.com/smpp/title~content=t713926090

Rotational dynamics and conformational kinetics in liquid crystals

A. Ferrarini[a]; A. Polimeno[a]; P. L. Nordio[a]
[a] Dipartimento di Chimica Fisica, Università degli Studi di Padova, Padova, Italy

To cite this Article Ferrarini, A. , Polimeno, A. and Nordio, P. L.(1993) 'Rotational dynamics and conformational kinetics in liquid crystals', Liquid Crystals, 14: 1, 169 — 184
To link to this Article: DOI: 10.1080/02678299308027310
URL: http://dx.doi.org/10.1080/02678299308027310

PLEASE SCROLL DOWN FOR ARTICLE

Full terms and conditions of use: http://www.informaworld.com/terms-and-conditions-of-access.pdf

This article may be used for research, teaching and private study purposes. Any substantial or systematic reproduction, re-distribution, re-selling, loan or sub-licensing, systematic supply or distribution in any form to anyone is expressly forbidden.

The publisher does not give any warranty express or implied or make any representation that the contents will be complete or accurate or up to date. The accuracy of any instructions, formulae and drug doses should be independently verified with primary sources. The publisher shall not be liable for any loss, actions, claims, proceedings, demand or costs or damages whatsoever or howsoever caused arising directly or indirectly in connection with or arising out of the use of this material.

LIQUID CRYSTALS, 1993, VOL. 14, NO. 1, 169–184

Invited Lecture

Rotational dynamics and conformational kinetics in liquid crystals

by A. FERRARINI, A. POLIMENO and P. L. NORDIO*
Dipartimento di Chimica Fisica, Università degli Studi di Padova,
2, Via Loredan, 35131 Padova, Italy

Two particular aspects of solute dynamics in ordered media are analysed on the basis of the solution of multivariate diffusion equations: the effects of the solvation dynamics on the rotational motions of dipolar probes in liquid crystal solvents, and the alteration of reaction pathways in isomerization kinetics caused by the solvent order. The introduction of a suitable solvent coordinate allows the interpretation of high frequency contributions in the rotational correlation functions observed by spectroscopic techniques, namely dielectric dispersion, IR and Raman spectroscopy, ESR lineshapes and optical Kerr effect. For molecular systems undergoing conformational changes, a method is offered to evaluate the modification of the torsional barriers resulting from the anisotropic torques modulated by the molecular shape changes along the reaction coordinate.

1. Introduction

The dynamical behaviour of molecules in liquid crystals is almost invariably described by means of stochastic equations where the environment enters as a continuous medium, exerting a frictional drag and the forces and torques responsible for the mesomorphic ordering [1]. The frictional effects are related to the macroscopic viscosity properties of the mesophase, while torques and forces are expressed in terms of anisotropic pseudo-potentials, whose expansion coefficients can be in principle determined by the experimental order parameters which characterize the static properties of the liquid crystal phase. In practice, complete information on the order parameters is not available, and so we must resort to maximum information entropy methods [2], or molecular field theories which provide a mean-field potential as a statistical average of pairwise interactions [3–5]. Alternatively, the anisotropic potential can be evaluated from models which account for the disturbance of the solvent order caused by solutes of particular shape [6, 7].

With these ingredients, the rotational and translational dynamics of rigid probe molecules dissolved in liquid crystals is rather well-understood. Thus, ESR lineshapes [8], selective NMR T_1 relaxation [9], or fluorescence depolarization experiments on solutes [1, 10] have been satisfactorily interpreted. Under some simplifying assumptions, the behaviour of the mesogen molecules themselves can also be rationalized [11]. Most mesogen molecules have flexible alkyl chains, and also the dynamical contributions of these internal motions can be taken into account, at a reasonable cost of computational effort [12, 13].

---

* Author for correspondence.

0267-8292/93 $10·00

In pure nematogens, NMR relaxation and dielectric dispersion data can be in general analysed quite easily, if in the latter case the monitoring electric field is taken parallel to the optical axis of the mesophase. With this geometry, reorientations of the molecular dipole component along the field direction require the passage over the barrier of the nematic potential, and so the dipole relaxation is hindered, and shifted to lower frequency with respect to the isotropic phase. Difficulties for the theoretical analysis arise in relation to the intriguing results obtained when the experimental techniques probe faster timescales, as in the case of dielectric dispersion with perpendicular alignment of the electric field [13–15], IR–Raman scattering spectroscopy [16], neutron scattering [17] or optical Kerr effect (OKE) [18] experiments. In all these cases, motions faster than expected appear to be revealed; in fact, values as high as 10^{11} for $D_{\parallel}$ in relatively viscous nematics are commonly reported. Motions faster than the typical values (10^8–10^{10}) of the rotational diffusion may originate from librations within instantaneous solvent cages, specific couplings with solvent coordinates, or internal motions if flexible molecules are considered, and it is therefore important to identify the relevant motional process.

Additional complications arise in the case of probe molecules undergoing conformational transitions [19]. This case is interesting because it provides a simple example of unimolecular reactions, and the theoretical description of the solvent effect on the kinetics can be very instructive.

The anisotropic environment is expected to have a two-fold influence on the conformational kinetics of a dissolved probe:

(1) an essentially static effect, the internal energy surface being altered by the mean-field potential;
(2) a dynamical coupling of solvent and reactive coordinates, which determines the reaction pathway according to the different time scale [20, 21].

With the aim of supplying a theoretical model able to provide answers, at a semiquantitative level, to all the questions posed above, we shall organize this paper as follows. In § 2 we shall describe a multivariate diffusion equation, in which some relevant solvent variables are included. We shall choose as solvent variables the fluctuating components of the macroscopic polarization, as dictated by the polar nature of the mesogenic molecules that we shall consider. We will show that high frequency components in the molecular orientational correlation function naturally appear in this way. In § 3 we shall consider the effect of the presence of the orientational mean-field potential on the conformational kinetics, and we shall discuss the role of specific solvent effects.

2. The model of solvation dynamics

The time evolution of the tumbling motion of a probe molecule in a liquid phase can be described when we are able to select the relevant set of dynamical coordinates which are likely to exhibit a relaxation behaviour in the time scale of the experimental observation. We shall consider a typical measure of dielectric relaxation for a dipolar fluid. The rotational coordinates (Euler angles Ω) for a single dipole are identified as the primary set of relevant coordinates. All other molecular degrees of freedom are supposed to be completely decoupled or too fast relaxing to effectively influence the time evolution of the dipole moment. Thus, vibrational degrees of freedom are excluded because they are too fast, and the translational ones are supposedly uncoupled, as is the case for cylindrical molecules in uniaxial phases.

In order to take into account the polar nature of the fluid, we assume that the dipole reorients inside an Onsager cavity, and so a relevant collective polarization coordinate is assumed to be the randomly fluctuating reaction field $\mathbf{X}(t)$ [22].

The time evolution of the conditional probability $P(\Omega,\mathbf{X},t)$ is taken as a Smoluchowski equation having the form [23]

$$(\partial/\partial t)P(\Omega,\mathbf{X},t)=-\hat{\Gamma}P(\Omega,\mathbf{X},t), \tag{1}$$

where

$$-\hat{\Gamma}=\hat{\mathbf{M}}\cdot\mathbf{D}_{\mathrm{R}}P_{\mathrm{eq}}(\Omega,\mathbf{X})\cdot\hat{\mathbf{M}}P_{\mathrm{eq}}^{-1}(\Omega,\mathbf{X})+(\partial/\partial\mathbf{X})\cdot\mathbf{D}_{\mathrm{S}}P_{\mathrm{eq}}(\Omega,\mathbf{X})\cdot(\partial/\partial\mathbf{X})P_{\mathrm{eq}}^{-1}(\Omega,\mathbf{X}). \tag{2}$$

In this equation, $\hat{\mathbf{M}}$ is the infinitesimal rotation operator, acting on the Ω sub-space and defined in the molecular frame, $(\partial/\partial\mathbf{X})$ is the gradient operator acting on the $\mathbf{X}$ sub-space and defined in the laboratory frame. The Boltzmann distribution $P_{\mathrm{eq}}(\Omega,\mathbf{X})$ is the form assumed by $P(\Omega,\mathbf{X},t)$ for $t\rightarrow\infty$ and is defined in terms of the potential energy function as

$$P_{\mathrm{eq}}(\Omega,\mathbf{X})=\exp[-V(\Omega,\mathbf{X})/k_{\mathrm{B}}T]/\langle\exp[-V(\Omega,\mathbf{X})/k_{\mathrm{B}}T]\rangle, \tag{3}$$

where the brackets denote an integral over all the states of the system; lastly, $\mathbf{D}_{\mathrm{R}}$ and $\mathbf{D}_{\mathrm{S}}$ are the diffusion tensor for the rotational and the solvent degrees of freedom, respectively. The potential energy for the overall system is given by the following expression [23]

$$V(\Omega,\mathbf{X})=V_0(\Omega)-\boldsymbol{\mu}(\Omega)\cdot\mathbf{X}+\tfrac{1}{2}\mathbf{X}\cdot\Xi^2\cdot\mathbf{X}. \tag{4}$$

The first contribution is present only when a liquid-crystalline phase is considered. For a typical nematic, we assume the usual Maier–Saupe [3] mean field

$$V_0(\Omega)=v\bar{P}_2P_2(\cos\beta), \tag{5}$$

where v is a strength parameter and $\bar{P}_2$ is the order parameter.

The second contribution defines the coupling between the molecular dipole and the polar environment, and we assume for it a classic dipole-field form. The dipole moment is written as

$$\boldsymbol{\mu}=\mu\mathbf{u}(\Omega), \tag{6}$$

and for simplicity, in the following calculations the unitary vector $\mathbf{u}$ is assumed to point along the z axis of the molecular frame fixed on the probe. This choice does not affect the conclusions which can be drawn from the model, although it simplifies a little the algebraic calculations.

The third term describes the potential energy for the fluctuating reaction field alone. The matrix Ξ^2 determines the fluctuation amplitudes, and it is taken diagonal in the laboratory frame of reference.

2.1. *Relation of dynamical parameters to macroscopic properties*

The potential and diffusion tensors parameters which appear in the above expressions can be evaluated, at least qualitatively, from simple hydrodynamic and electrostatic considerations. Let us first recall the case of a spherical molecule in isotropic liquids [23], when the potential strength for the mean field parameter v is obviously set to zero. The diffusion tensor for the rotational motion is replaced by the scalar

$$D_{\mathrm{R}}=1/\tau_{\mathrm{R}}, \tag{7}$$

where τ_R is the (unique) rotational decay time. The potential and diffusion parameters concerning the stochastic field are evaluated from the knowledge of the correlation function for **X** in the absence of coupling with the dipole probe

$$\overline{\mathbf{X}(0)\cdot\mathbf{X}(t)}=\frac{3k_BT}{\Xi^2}\exp\left(-\frac{D_S\Xi^2}{k_BT}t\right), \tag{8}$$

which can be compared with the standard form derived on the basis of dielectric theories for the reaction field

$$\overline{\mathbf{X}(0)\cdot\mathbf{X}(t)}=\frac{3k_BT}{a^3}\left(\frac{\epsilon_0-1}{\epsilon_0+\frac{1}{2}}-\frac{\epsilon_\infty-1}{\epsilon_\infty+\frac{1}{2}}\right)\exp\left(-\frac{t}{\tau_S}\right) \tag{9}$$

to obtain physical interpretations for the scalars Ξ^2 and D_S:

$$\frac{1}{\Xi^2}=\frac{1}{a^3}\left(\frac{\epsilon_0-1}{\epsilon_0+\frac{1}{2}}-\frac{\epsilon_\infty-1}{\epsilon_\infty+\frac{1}{2}}\right), \tag{10}$$

$$D_S\Xi^2=k_BT/\tau_S. \tag{11}$$

In these expressions a, ϵ_0 and ϵ_∞ are the radius of the spherical Onsager cavity, and the static and optical dielectric constants, respectively. Finally, τ_S is proportional to the dielectric relaxation time τ_D

$$\tau_S=\frac{2\epsilon_\infty+1}{2\epsilon_0+1}\tau_D. \tag{12}$$

To conclude, we should remark that $\tau_D=1/2D_R$, and that information on the correlation function $\overline{\mathbf{X}(0)\cdot\mathbf{X}(t)}$ is obtained from the knowledge of time-dependent Stokes shifts [22].

A simple way to generalize the previous formulas to anisotropic cases is to choose v different from zero and to substitute the scalars with tensors. Therefore, we shall assume the rotational diffusion tensor for the elongated mesogen molecule to be diagonal and axially symmetric in the molecular frame

$$\mathbf{D}_R=\begin{pmatrix} D_R^{\perp} & 0 & 0 \\ 0 & D_R^{\perp} & 0 \\ 0 & 0 & D_R^{\parallel} \end{pmatrix} \tag{13}$$

while the polarization diffusion and fluctuations tensors are taken diagonal in the laboratory frame with the Z axis coincident with the optical axis of the uniaxial mesophase:

$$\mathbf{D}_S\Xi^2=k_BT\begin{pmatrix} 1/\tau_S^{\perp} & 0 & 0 \\ 0 & 1/\tau_S^{\perp} & 0 \\ 0 & 0 & 1/\tau_S^{\parallel} \end{pmatrix} \tag{14}$$

$$\Xi=\begin{pmatrix} \Xi_{\perp} & 0 & 0 \\ 0 & \Xi_{\perp} & 0 \\ 0 & 0 & \Xi_{\parallel} \end{pmatrix}. \tag{15}$$

The perpendicular and parallel components of $\mathbf{D}_S$ and Ξ are simply obtained by expressions similar to equations (10), (11) and (12), by substituting ϵ_0, ϵ_∞ with the principal components $\epsilon_0^{(\perp,\,\parallel)}$ and $\epsilon_\infty^{(\perp,\,\parallel)}$ measured in uniaxial phases. Obviously, this is a very rough way of treating anisotropy, especially since we maintain a spherical form for the Onsager cavity and we neglect hydrodynamic interactions, although more sophisticated treatments are available [24, 25]. However, we can see that even this simple model allows us to extract the important physical factors which determine the relaxation behaviour of the system. For instance, the coupling of the molecular dipole with the solvent reaction field provides naturally an additional retarding torque for the dipole reorientation, termed as dielectric friction [22, 23].

Note that the definition of the order parameter is somewhat modified with respect to the usual one-body treatments, since we have to take into account the average over all the relevant coordinates of the system

$$\bar{P}_2=\langle P_2(\cos\beta)P_{\mathrm{eq}}\rangle=\frac{\int d\Omega\int d\mathbf{X}\,P_2(\cos\beta)\exp\left[-V(\Omega,\mathbf{X})/k_{\mathrm{B}}T\right]}{\int d\Omega\int d\mathbf{X}\exp\left[-V(\Omega,\mathbf{X})/k_{\mathrm{B}}T\right]}. \tag{16}$$

The anisotropy in the tensor Ξ has the effect of introducing an additional orienting term in the mean field potential, plus a stabilization energy term

$$v_0=\frac{\mu^2}{3}\left(\frac{1}{\Xi_\parallel^2}-\frac{1}{\Xi_\perp^2}\right), \tag{17}$$

$$\Delta E_{\mathrm{S}}=\frac{\mu^2}{6}\left(\frac{1}{\Xi_\parallel^2}+\frac{2}{\Xi_\perp^2}\right). \tag{18}$$

We are finally left with the following parameters: the energetics is defined by v (mean field potential), v_0 and ΔE_{S}, the dynamics is determined by the two rotational diffusion tensor components $D_{\mathrm{R}}^{\perp}$, $D_{\mathrm{R}}^{\parallel}$, and the two solvent relaxation times $\tau_{\mathrm{S}}^{\perp}$, $\tau_{\mathrm{S}}^{\parallel}$.

2.2. *Dielectric relaxation in polar nematics*

We are interested in evaluating correlation functions for the dipole component relaxations, i.e. $\overline{\mu_Z(0)\mu_Z(t)}$ (relaxation of the dipole along the Z axis of the lab frame) and $\overline{\mu_X(0)\mu_X(t)}=\overline{\mu_Y(0)\mu_Y(t)}$ (relaxation of the dipole in the XY plane of the lab frame). These are related to correlation functions of first rank Wigner functions in Ω [26].

The numerical calculations are performed by the following sequence of operations:

(1) symmetrization of the time evolution operator, which consists in making the operator $\hat{\Gamma}$ hermitean by the unitary transformation

$$\tilde{\Gamma}=P_{\mathrm{eq}}^{-1/2}\hat{\Gamma}P_{\mathrm{eq}}^{1/2}, \tag{19}$$

the eigenvalues of $\tilde{\Gamma}$ being the same as those of $\hat{\Gamma}$;

(2) representation in matrix form of the symmetrized operator on a suitable orthonormal set of basis functions;

(3) representation of the observables (dipole components) in vectorial form on the same basis set;

(4) application of iterative algorithms, such as Lanczos, on the large sparse matrix obtained in step (1) with the initial vector given by step (2), in order to transform the matrix into tridiagonal form [27];

(5) evaluation of the spectral densities (Fourier–Laplace transforms of the correlation functions) directly from the tridiagonal matrix as a continuous fraction, or selection of the most relevant eigenvalues (time decay constants) from a QR [27] diagonalization of the tridiagonal matrix.

Details of the algebraic procedure are given elsewhere [27, 28]. The basis functions have been taken as the direct product of normalized Wigner matrices in Ω and normalized Hermite functions in X_i, Cartesian component of the reaction field. The basis set can be written in bracket form as

$$|JMK;\ n_1n_2n_3\rangle=|JMK\rangle|n_1\rangle|n_2\rangle|n_3\rangle, \tag{20}$$

$$|JMK\rangle=[(2J+1)/8\pi^2]^{1/2}\mathscr{D}^J_{MK}{}^*(\Omega), \tag{21}$$

$$|n_i\rangle=\mathrm{He}_{n_i}(X_i)\exp(-X_i^2/4)/(2\pi)^{1/4}. \tag{22}$$

Having chosen the unitary vector $\mathbf{u}$ of the dipole moment along the z axis of the molecular frame, we need to compute the following correlation functions, already expressed in terms of the basis functions

$$G^1_{00}(t)\equiv G_{\parallel}(t)=\langle(100;\ 000)\ P^{1/2}_{\mathrm{eq}}|\exp(-\tilde{\Gamma}t)|(100;\ 000)P^{1/2}_{\mathrm{eq}}\rangle, \tag{23}$$

$$G^1_{10}(t)\equiv G_{\perp}(t)=\langle(110;\ 000)\ P^{1/2}_{\mathrm{eq}}|\exp(-\tilde{\Gamma}t)|(110;000)P^{1/2}_{\mathrm{eq}}\rangle. \tag{24}$$

The functions $G_{\parallel}(t)$ and $G_{\perp}(t)$ allow us to describe relaxation experiments performed with the electric field parallel or perpendicular to the optical axis of the mesophase. It follows from the chosen probe geometry that only $D^{\perp}_{\mathrm{R}}$ enters in determining the time decays of both $G_{\parallel}(t)$ and $G_{\perp}(t)$. By analogy with equation (7) we shall continue to define a characteristic time $\tau_{\mathrm{R}}=1/D^{\perp}_{\mathrm{R}}$.

For actual calculations we have made reference to the molecular system 4-*n*-heptyl-4′-cyanobiphenyl (7CB) in the nematic phase, for which all the necessary dielectric data are available [29]. The static and optical dielectric constant measured with a field parallel to the director $\mathbf{n}$ are $\epsilon^{\parallel}_0=16{\cdot}3$ and $\epsilon^{\parallel}_{\infty}=3{\cdot}1$, respectively; if the field is perpendicular the measured values are $\epsilon^{\perp}_0=5{\cdot}9$ and $\epsilon^{\perp}_{\infty}=2{\cdot}5$. The reported dielectric relaxation times are $\tau^{\parallel}_{\mathrm{D}}\sim 32$ ns and $\tau^{\perp}_{\mathrm{D}}\sim 2$ ns.

The ratio $\Xi^2_{\perp}/\Xi^2_{\parallel}$ is then evaluated to be 1·2, and so for this system the ratio $|v_0/\Delta E_{\mathrm{S}}|$ has a value of about 0·1. In terms of the rotational time τ_{R} the dielectric relaxation times calculated by means of one-body models [26] turn out to be $\tau^{\perp}_{\mathrm{D}}\sim\tau_{\mathrm{R}}$ and $\tau^{\parallel}_{\mathrm{D}}\sim 10\tau_{\mathrm{R}}$, in agreement with the experimental values reported above. It follows from equation (12), modified by the inclusion of the suitable dielectric tensor components, that the solvent relaxation times are roughly given by $\tau^{\perp}_{\mathrm{S}}\sim 0{\cdot}5\tau^{\perp}_{\mathrm{D}}\sim 0{\cdot}5\tau_{\mathrm{R}}$, and $\tau^{\parallel}_{\mathrm{S}}\sim 0{\cdot}2\tau^{\parallel}_{\mathrm{D}}\sim 2\tau_{\mathrm{R}}$. These estimates suggest that the dynamical effect of anisotropy, i.e. its influence on the diffusion time scale by means of dielectric friction, is likely to be more relevant than its static effects. This is in accordance with MD simulations [30] and NMR experiments [31] in which the aligning effect of dipolar forces in nematics is found negligible, when compared with steric interactions effects. For a typical nematic at 50°C one measures an order parameter of 0·6 which corresponds, in standard mean field theory, to a value of $-v/k_{\mathrm{B}}T$ close to 5. Therefore we shall neglect the v_0 term because it is expected to be small compared with this value.

The spectral densities relative to the correlation functions $G(t)$ given in equations (23) and (24) have been computed for several sets of parameters, and one of the most significant results is shown in figure 1, in the form of a Cole–Cole plot, i.e. with the imaginary part L'' versus the real part L' of the Fourier–Laplace transform

$$L(\omega)=-\int_0^{\infty}dt\exp(-\mathrm{i}\omega t)\frac{d}{dt}G(t). \tag{25}$$

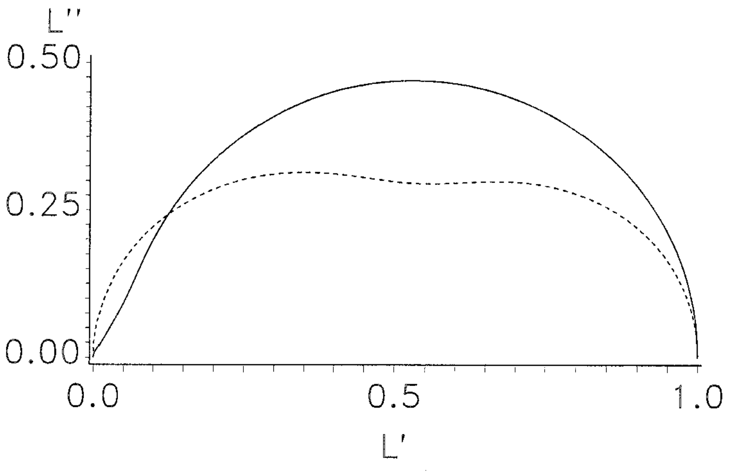

Figure 1. Cole–Cole plots for the correlation function of the molecular dipole components parallel (full line) and perpendicular (dotted line) to the director, calculated for the nematic phase of 7CB. Energetic and dynamical parameters are given in the text.

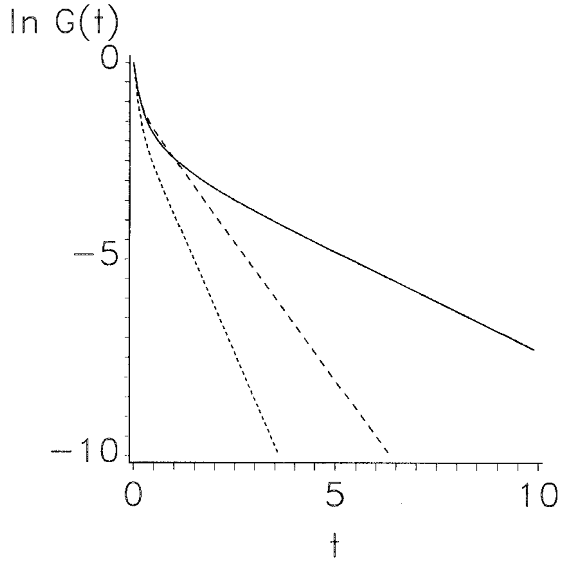

Figure 2. Semilogarithmic plot of correlation functions for the second rank Wigner components $\mathscr{D}^2_{00}$ (full line), $\mathscr{D}^2_{10}$ (dashed line) and $\mathscr{D}^2_{20}$ (dotted line), calculated for the nematic phase of 7CB.

We have taken the values $\tau_S^\perp/\tau_R = 0{\cdot}5$, $\tau_S^\parallel/\tau_R = 2$, and a stabilization energy ΔE_S given by $2k_BT$. Complete convergence at the fourth figure for all relevant eigenvalues is achieved for matrix dimensions of about 3000, the number of Lanczos steps required to efficiently tridiagonalize the matrix being always less than 50. The Cole–Cole plot for the first rank correlation functions shows a dramatic departure from simple monoexponential decay for the perpendicular component. The dominant decay time for the parallel component is still the eigenvalue related to the jump motion between the two minima of the orientational potential, while the decay of the perpendicular component results from the molecule diffusive librations within the minima, strongly intermixed with the solvent decay times.

We see therefore that with relatively low values of the dipole stabilization energy, drastic flattening of the Cole–Cole plots is predicted only for dipole relaxation experiments with perpendicular arrangements of the electric field. These results are in complete agreement with the experimental observations [14], and since conformational motions of the alkyl chains are unable to account for so large effects [13], the shape of the Cole–Cole plots in nematics may be taken as a strong evidence of the existence of polarization fluctuations in these systems.

Other experiments can also probe fast relaxing components resulting from the couplings with the solvent. Figure 2 displays the semilogarithmic plot of normalized time correlation functions of second rank Wigner components, relevant for the interpretation of Raman or OKE experiments, and the fast decay at short times is clearly exhibited.

This dynamical behaviour may also be the origin of the frequency dependence of the diffusion tensor of spin probes monitored by ESR experiments, implying the existence of local torques [32] relaxing slowly with respect to the timescale of the solvent cages, which give rise to far infrared spectra, but still fast compared with the orientational tumbling.

3. Effect of the nematic order on isomerization kinetics

The exploitation of ordered media to alter the activation parameters and the kinetic pathways in chemical reactions has been pursued by several researchers, and the reader is referred to a review article by Weiss [33] for an exhaustive illustration of papers related to this argument. A number of papers have been devoted to the understanding of the solute–solvent interactions which influence unimolecular reactions in mesophases. For a rotameric molecule which does not present polar character, we generally assume that the rate constants in isotropic phases depend essentially upon the internal torsional potential, the interactions with the solvent having only minor effects. This is no longer true in liquid crystal phases, where the molecules experience anisotropic torques of the order of magnitude of several $k_B T$ units, which tend to orient the various molecular moieties and can compete with the torsional potential in determining both the stable states and the interconversion rates. Evidence actually exists that solvent order can control conformational kinetics when extensive shape changes in the transition state are involved.

Typical examples of simple systems whose conformational kinetics has been studied in ordered phases are provided by the biphenyl, 1,1′-binaphthyl (BN), and stilbene molecules. The case of the biphenyl isomerization has been extensively treated elsewhere [19], and only a few remarks shall be added here. The thermal racemization of BN, depicted in figure 3, has been experimentally investigated in a series of isotropic and nematic solvents [34]. On a qualitative ground, we expect the interconversion rate to increase in ordered phases, because the solvent order forces the molecule in the planar configuration, which corresponds to the transition state configuration. Since this configuration implies a higher ordering for both the BN molecule and the surrounding mesogen molecules, a relatively large decrease of the total entropy is also expected, in agreement with the observations. Lastly, the isomerization process of *cis*-stilbene is apparently a case in which the prediction of the effects of the nematic order is contradicted by the experiments [33].

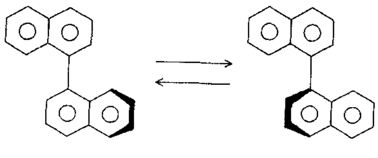

R-(−)-BN S-(+)-BN

Figure 3. Interconversion of the optical isomers of 1,1′-binaphthyl across the *trans* barrier.

3.1. *Orientational and torsional potential*

In order to describe the kinetics of isomerization for molecules in ordered phases, we need first a detailed knowledge of the potential that they experience. For a molecule with a single internal degree of freedom in a nematic uniaxial phase, such a potential can be written as $V(\Omega, \varphi)$, where φ is the torsional angle and Ω are the Euler angles for the transformation from the laboratory frame, with the Z axis along the mesophase director **d**, to a molecular reference system, fixed in one of the rigid subunits of the molecule. We start by writing the potential as

$$V(\Omega, \varphi) = V^{\text{int}}(\varphi) + V^{\text{ext}}(\Omega, \varphi) \tag{26}$$

where $V^{\text{int}}(\varphi)$ and $V^{\text{ext}}(\Omega, \varphi)$ represent the torsional, or internal, and the orientational, or external contribution, respectively.

The first term is determined exclusively by intramolecular interactions, and it will be taken from data available in the literature.

The other contribution, $V^{\text{ext}}(\Omega, \varphi)$, is calculated according to a model we have recently developed to describe the anisotropic field acting on molecules of arbitrary shape in uniaxial liquid crystal phases [7]. It is worth summarizing here the basic features of the treatment. It belongs to the so-called 'shape' models which, recognizing the repulsion intermolecular interactions as the dominant, although not the only orienting mechanism, try to relate the anisotropic torques experienced by the molecules with their steric arrangement. By analogy with the surface anchoring potential which determines the orientation of a macroscopic particle in a bulk nematic [35], we write the external potential as

$$V^{\text{ext}}/k_{\text{B}}T = \varepsilon \int_S dS P_2(\cos \psi_{\mathbf{n}_{\text{S}},\mathbf{d}}), \tag{27}$$

where the integral is defined over the S of the particle. $P_2(\cos \psi_{\mathbf{n}_{\text{S}},\mathbf{d}})$ is a second order Legendre polynomial, $\psi_{\mathbf{n}_{\text{S}},\mathbf{d}}$, being the angle between the normal $\mathbf{n}_{\text{S}}$ to the surface and the director **d**, which depends upon the surface element considered and the internal angle φ. The parameter ε gives the strength of the orienting potential, taken as positive for normal calamitic nematics, so that the mesophase director tends to align parallel to the surface at each surface element. The surface of the molecule is defined by describing the molecule as an array of van der Waals overlapping spheres, centred at the atomic positions. In order to implement the calculation of the orienting potential, it is convenient to rewrite equation (27) by making use of the spherical harmonics addition theorem [36]. The following expression is derived

$$V^{\text{ext}}/k_{\text{B}}T = -\varepsilon \sum_m T^{2,m*} C_{2,m}(\beta, \gamma), \tag{28}$$

where $C_{2,m}$ are modified spherical harmonics and $T^{2,m}$ are the irreducible spherical components of a rank two, symmetric and traceless interaction tensor **T**, defined as

$$T^{2,m} = -\int_S dSC_{2,m}(\theta, \phi). \qquad (29)$$

The angles (β, γ) and (θ, ϕ) give the orientation in the molecular frame of the director **d** and of the unit vector $\mathbf{n}_S$, respectively.

The spherical irreducible components of the tensor **T** can be calculated at discrete values of the torsional angle φ, and the data are then interpolated by a Fourier series, to derive analytical expressions which can be efficiently implemented [19].

3.2. *Isomerization dynamics*

The kinetics of the isomerization process is investigated by making use again of the formalism of multivariate diffusion equations. In fact, since we assume the viscosity of the medium high enough to quench effectively the angular velocities, we can restrict ourselves to a Smoluchowski equation for the torsional (φ) and the orientational (Ω) variables, which are coupled by the orienting potential, as we have already seen, and by frictional effects. In fact, the frictional forces opposing both the overall molecular reorientations and the conformational transitions depend upon the actual molecular shape. The time evolution of the torsional–orientational distribution function $P(\Omega, \varphi, t)$ is then governed by the diffusion operator

$$-\hat{\Gamma} = \nabla \cdot \mathbf{D}(\varphi) P_{\mathrm{eq}}(\Omega, \varphi) \cdot \nabla P_{\mathrm{eq}}^{-1}(\Omega, \varphi). \qquad (30)$$

In this equation ∇ denotes a suitable gradient operator acting on all variables, $\nabla = (M_x, M_y, M_z, \partial/\partial\varphi)$, and $P_{\mathrm{eq}}\,(\Omega, \varphi)$ is the equilibrium distribution function, defined by

$$P_{\mathrm{eq}}(\Omega, \varphi) = \exp\left[-V(\Omega, \varphi)/k_{\mathrm{B}}T\right] / \langle \exp\left[-V(\Omega, \varphi)/k_{\mathrm{B}}T\right] \rangle. \qquad (31)$$

If the torsional barrier is relatively low, up to a few $k_{\mathrm{B}}T$ units, conformational transitions occur on the same time scale of the reorientational motions. The couplings between the two kinds of motions, determined by the conformation dependence of both the diffusion tensor and the orienting torques, must be taken into account, and therefore the full four dimensional diffusion equation given by equation (30) must be solved.

When the torsional barriers are high, as is the case of BN for which values of $67\,\mathrm{kJ\,mol^{-1}}$ or more are assigned [34], the conformational process is strongly hindered and an effective time scale separation with the rotational motions occurs. Under this condition, a projection procedure on the time evolution operator can be performed, aimed to eliminate the fast variables in the calculation of the transition rate. The reduced diffusion equation in the slow coordinate φ is therefore

$$(\partial/\partial t) P(\varphi, t) = -\hat{\Gamma}_{\varphi} P(\varphi, t) \qquad (32)$$

and

$$-\hat{\Gamma}_{\varphi} = (\partial/\partial\varphi) D_{\varphi} P(\varphi) (\partial/\partial\varphi) D_{\varphi} P^{-1}(\varphi), \qquad (33)$$

where D_φ is the diffusion coefficient for the torsional motion, and the distribution function $P(\varphi)$ is given by

$$P(\varphi)=\int d\Omega P_{\mathrm{eq}}(\Omega,\varphi). \tag{34}$$

The reduced distribution $P(\varphi)$ can be thought of as deriving from an effective potential $V^{\mathrm{eff}}(\varphi)$, defined as

$$V^{\mathrm{eff}}(\varphi)=-k_{\mathrm{B}}T\ln P(\varphi). \tag{35}$$

As long as this potential exhibits high barriers, the kinetic parameters can be derived by asymptotic solutions of the diffusion equation [37, 38]. So, in the case of a bistable potential characterized by two equivalent minima in the regions $0<\varphi<\pi$ and $\pi<\varphi<2\pi$, the rate constant for the interconversion process across the barrier at $\varphi=0°$ is accurately calculated as

$$k=2D_\varphi\left[\int_{-\varphi_m}^{\varphi_m} d\varphi P^{-1}(\varphi)\right]^{-1}, \tag{36}$$

where $\pm\varphi_{\mathrm{m}}$ correspond to the location of potential minima. This result is a generalization of the Kramers expression [39] for the rate constants of activated processes.

3.3. *Numerical examples*

The projection procedure leading to equations (33) and (35) is valid only under the condition of timescale separation between internal and overall rotations. If this condition is not fulfilled, the kinetic constants calculated by equation (36) are in error, and also the definition of V^{eff} may be misleading. In fact, if the rotational motions were slower than the conformational transitions, the rate determining step of the conformational process could not be simply identified as the passage across the barrier of the internal potential, but rather it should be associated to the approaching of the saddle point along the slow coordinate [20, 21]. In any case, the calculation of the orientational order parameters requires the full distribution function $P_{\mathrm{eq}}(\Omega,\varphi)$.

Having payed the proper attention to the timescale separation condition, it is interesting to notice that if we write

$$V^{\mathrm{eff}}(\varphi)=V^{\mathrm{int}}(\varphi)+\delta V^{\mathrm{aniso}}(\varphi) \tag{37}$$

with $\delta V^{\mathrm{aniso}}$ the correction determined by the anisotropic environment, the evaluation of the last term does not require the knowledge of V^{int}. In fact, within the limits of validity of equation (26) we have

$$\delta V^{\mathrm{aniso}}(\varphi)=-k_{\mathrm{B}}T\ln\int d\Omega\exp\left[-V^{\mathrm{ext}}(\Omega,\varphi)/k_{\mathrm{B}}T\right]. \tag{38}$$

The corrections $\delta V^{\mathrm{aniso}}$ for biphenyl, 1,1′-binaphthyl and stilbene are displayed in figure 4. The torsional angle has been taken as $\varphi=0°$ for planar biphenyl, and for the *trans* configurations of BN and stilbene. The calculation of V^{ext} has been performed with the methods described in section 3.1, by taking a value ε of $0{\cdot}1\,\text{Å}^{-2}$ which provides a reasonable ordering ($S_{zz}=0{\cdot}5\div0{\cdot}6$) for the solutes in nematics. In the calculation of the interaction tensor **T** both carbon atoms and CH groups are described as spheres of radius equal to 2 Å. The aromatic rings are taken as regular hexagons, with all bond

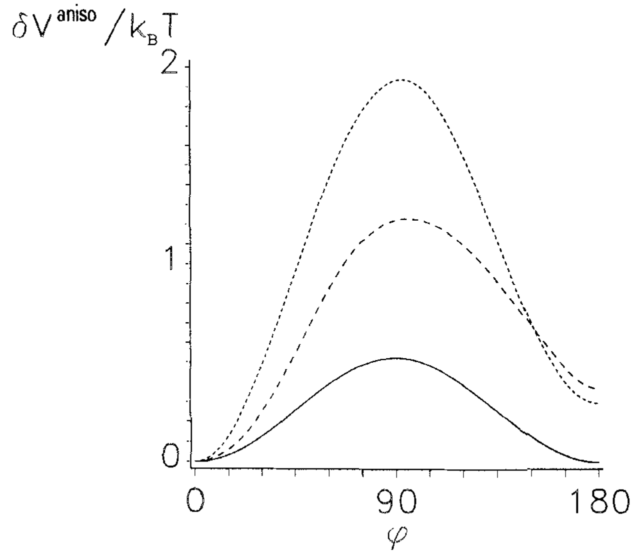

Figure 4. Corrections to the internal potential due to the nematic environment, calculated for biphenyl (full line), stilbene (dashed line) and binaphthyl (dotted line). The shape model discussed in the text has been used to evaluate the dependence upon the molecular conformation of the anisotropic potential.

lengths equal to 1·395 Å. For the sake of simplicity, the same value of 1·52 Å has been assigned in all cases to the bond involved in the rotational isomerization process.

Figure 4 clearly shows that the planar configurations are stabilized for all three molecular systems. In the case of BN, the planar *trans* configuration corresponds to the transition state, the stable isomers having the naphthalene moieties almost perpendicular to each other. As a consequence, the effect of the nematic order is to lower the barrier at the transition state, and therefore to accelerate the transition rate. The opposite conclusion is true for stilbene, where the stable forms are planar, and the transition state corresponds to an orthogonal arrangement of the phenyl rings. In this case, the stabilization of the planar forms implies an increase of the barrier height. The situation is slightly more complicated for biphenyl, where the isomerization involves the passage over barriers at $\varphi=0$ and $\varphi=\pi/2$ [19], and so the barrier at $\varphi=0$ will be lowered, while the barrier at $\varphi=\pi/2$ will increase.

In any case, the largest effect is observed for the BN molecule, where a decrease of about 2 k_BT units of the potential barrier is predicted. For geometrical reasons this molecule appears to be the most appropriate to investigate the kinetic effects of a nematic field. This is clearly not the case for biphenyl, which uniaxial phases tend to align with the para axis along the director, so that the latter can lie on both ring planes, irrespective of the torsional angle. This means that, at least for the energetically favoured molecular orientations, torsional and orientational potential are not coupled. The coupling is expected to become larger as the tilt angle between the para axis and the director increases, but such orientations are statistically less important. It is not so easy to predict how the binaphthyl molecule will be accommodated in a nematic phase but, because of its shape, its preferred orientation will markedly depend upon the value of the torsional angle. The relevance of the coupling can only be evaluated by numerical calculations.

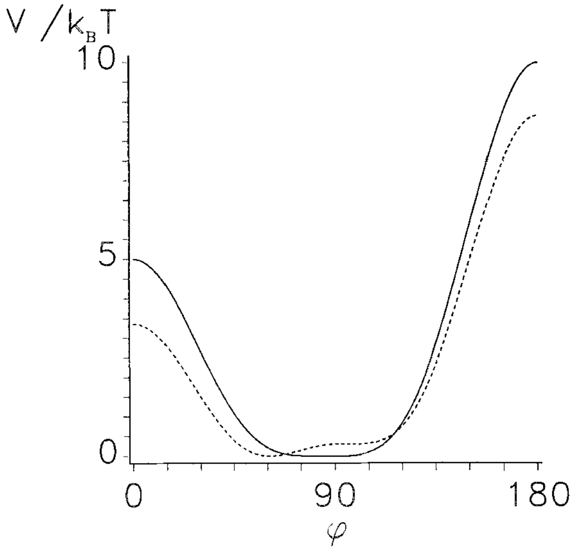

Figure 5. Alteration of the torsional potential profile for a BN-like molecule, due to the nematic environment. The full and dotted line represent the torsional potential in the isotropic and nematic phase, respectively. In order to visualize the effect, equation (39) with $\Delta = 5$, instead of the more realistic value $\Delta = 30$, has been used.

According to *ab initio* calculations [40] and molecular mechanics results [41], the ground state of binaphthyl is characterized by a torsional potential which is shallow in a wide range around the perpendicular conformation. In correspondence to the planar geometries there are two barriers, the higher one for the *cis* conformation, because of severe steric interactions. It follows that the stable conformers are predicted to be strongly non-planar, and a variety of values are possible for the twist angle, which is expected to be influenced by substituents which may be attached to the aromatic rings, and by specific interactions with the solvent.

The form of the potential for BN has been expressed by the following trigonometric expansion

$$V^{\mathrm{int}}(\varphi)/k_{\mathrm{B}}T = \Delta(-0{\cdot}75\cos\varphi + 1{\cdot}5\cos 2\varphi - 0{\cdot}25\cos 3\varphi + 0{\cdot}36\cos 4\varphi)/2, \qquad (39)$$

where Δ gives the height of the *trans* barrier.

The modification of the torsional potential profile of BN due to the anisotropic torques exerted by a nematic environment is shown in figure 5, where the appropriate contribution $\delta V^{\mathrm{aniso}}$ has been added to the internal potential given by equation (39). The unrealistically low value for Δ of 5 has been adopted in order to visualize the effect, that otherwise would be barely perceptible if the more realistic value for Δ of 30, suggested by the experimental data of [34] were used. In both cases, however, the same increase by a factor of about e^2 is obviously predicted for the isomerization rate.

When the value for Δ of 30 is assumed for the potential barrier, the rate constant for the conformational transition in isotropic phase at temperature T (K) and viscosity η (cP) can be calculated after evaluating D_φ from the physical dimensions of the BN molecule [19], and it is found to be

$$k_{\mathrm{iso}} \approx 8 \times 10^{-5}\, T/\eta \qquad (40)$$

In a nematic phase at the same temperature and viscosity, the rate constant is found to be faster by a factor of about 6, which roughly corresponds to that expected factor. It is interesting to realize that the isomerization of BN in the ground state occurs at a rate which is $12 \div 13$ orders of magnitude slower than the corresponding photoisomerization process, which involves the first electronically excited state of the molecule [19].

The order parameters of BN in nematics have also been calculated, with the value for ε of 0·1 Å^{-2} used to obtain the results shown in figures 4 and 5. By taking the z axis along the 1–1′ bond, and the y axis along the C_2 symmetry axis, the only symmetry element preserved by the conformational change, the non-vanishing ordering matrix elements are $S_{xx} = -0{\cdot}27$, $S_{yy} = -0{\cdot}31$, $S_{zz} = 0{\cdot}58$ and $S_{xz} = 0{\cdot}10$. For the rigid configuration having the naphthalene rings perpendicular to each other, we would have $S_{xx} = S_{yy} = -S_{zz}/2$ and $S_{xz} = 0$.

As a general conclusion, it appears that the isomerization kinetics may be significantly, but not drastically modified by the nematic ordering. The contradictory results for the *cis* stilbene isomerization probably reflect the modest effect expected in this case. Larger effects may result in more ordered phases, such as smectics. In fact, with an order parameter $S_{zz} \simeq 0{\cdot}8$ an effective decrease of 6 k_BT units is calculated for BN, implying an increase by a factor of 400 of the isomerization rate constant with respect to analogous isotropic conditions.

4. Concluding remarks

The molecular systems undergoing conformational changes, considered in § 3, are non-polar in character and therefore a single particle approach for the description of the internal kinetics is well-justified. Were the conformational transitions accompanied by changes in polarity, inclusion of the coupling with solvent coordinates as described in § 2 would be necessary. This situation generally arises in connection with photoisomerizations involving twisted intramolecular charge transfer (TICT) processes. A large amount of work has been devoted to study this aspect of the solvation dynamics in ordinary solvents [42], but surprisingly no attempt of exploiting in the same context the dynamical features of anisotropic solvents appears to have been carried out. A notable exception is the case of 9,9′-bianthryl (BA), whose spectroscopic behaviour has been investigated in micelles and lamellar phases [43]. BA provides a remarkable example of a molecular system, non-polar in the ground state, which exhibits an electron transfer in the excited state, promoted by polar solvents without significant conformational changes [44]. In fact, the two anthracene moieties assume a nearly orthogonal configuration, in both the ground and excited state of BA, in order to minimize the steric effects. In non-polar solvents, the absorption and emission spectra are therefore very similar to those of anthracene itself. Polar media, however, stabilize the charge transfer (CT) states obtained by excitation of an electron from the highest occupied molecular orbital of a ring to the lowest non-occupied orbital of the other, and so the fluorescence spectra exhibit a marked red-shift. Although the two CT structures of opposite polarity are degenerate in the isolated BA molecule, instantaneous polarization fluctuations break the symmetry inducing an effective electron transfer. The kinetics of the electron transfer, and of the consequent time dependent Stokes shift of the fluorescence emission, is therefore controlled by the solvent polarization fluctuations.

If BA is dissolved in microetherogeneous media, such as micelle samples, because of the hydrophobic character of the aromatic molecules they are expected to be preferentially located in the micellar cores. Molecules excited by a laser pump can then diffuse to the water interface, where the increase of the polarity induces the electron transfer. Under these conditions, the bathochromic shift of the fluorescence emission occurs on a timescale which is determined by the translation diffusion of the BA across the micelle dimensions. Such a mechanism for the time dependent Stokes shift is reminiscent of a spin relaxation effect caused in smectic A phases by translations across regions of non-uniform ordering [45], and therefore it can be analysed in a similar way.

This work has been supported by the Italian Ministry of the University and the Scientific and Technological Research, and in part by the National Research Council through its Centro Studi sugli Stati Molecolari. The authors acknowledge G. J. Moro for enlightening comments, and Professors C. Zannoni and G. R. Luckhurst for discussions on the conformational potential in flexible molecules.

References

[1] Ferrarini, A., Moro, G. J., and Nordio, P. L., 1993, *The Molecular Dynamics of Liquid Crystals*, edited by G. R. Luckhurst and C. Veracini (Kluwer), Chap. 3 (in the press).

[2] Berardi, R., Spinozzi, F., and Zannoni, C., 1992, *J. chem. Soc. Faraday Trans.*, **88**, 1863.

[3] Maier, W., and Saupe, A., 1959, *Z. Naturf.* (*a*), **14**, 882; *Ibid.*, **15**, 287.

[4] Humphries, R. L., James, P. G., and Luckhurst, G. R., 1972, *J. chem. Soc. Faraday Trans. II*, **68**, 1031.

[5] Luckhurst, G. R., Zannoni, C., Nordio, P. L., and Segre, U., 1975, *Molec. Phys.*, **30**, 1345.

[6] Zimmerman, D. S., Li, Y., and Burnell, E. E., 1991, *Molec. Crystals liq. Crystals*, **203**, 61.

[7] Ferrarini, A., Moro, G. J., Nordio, P. L., and Luckhurst, G. R., 1992, *Molec. Phys.*, **77**, 1.

[8] Freed, J. H., 1987, *Rotational Dynamics of Small and Macromolecules in Liquids*, edited by Th. Dorfmüller and R. Pecora (Springer), p. 89.

[9] Emsley, J. W., and Veracini, C. A. (editors), 1985, *NMR in Liquid Crystals* (Reidel).

[10] Arcioni, A., Bertinelli, F., Tarroni, R., and Zannoni, C., 1990, *Chem. Phys.*, **143**, 259.

[11] Beckmann, P. A., Emsley, J. W., Luckhurst, G. R., and Turner, D. L., 1986, *Molec. Phys.*, **59**, 97.

[12] Ferrarini, A., Moro, G. J., and Nordio, P. L., 1990, *Liq. Crystals*, **8**, 593.

[13] Ferrarini, A., Nordio, P. L., and Moro, G. J., 1991, *Molec. Crystals liq. Crystals*, **198**, 159.

[14] Wacrenier, J. M., Druon, C., and Lippens, D., 1981, *Molec. Phys.*, **43**, 97.

[15] Ratna, B. R., and Shashidhar, R., 1977, *Molec. Crystals liq. Crystals.*, **42**, 185.

[16] Rosi, B., Fontana, M. P., Dozov, I., and Kirov, N., 1987, *Phys. Rev.* A, **36**, 2879.

[17] Cvikl, B., and Dahlborg, U., 1984, *Molec. Crystals liq. Crystals*, **114**, 79.

[18] Deeg, F. W., Greenfield, S. R., Stankus, J. J., Newell, V. J., and Fayer, M. D., 1990, *J. chem. Phys.*, **93**, 3503.

[19] Ferrarini, A., and Nordio, P. L., 1992, *J. chem. Soc. Faraday Trans.*, **88**, 1733.

[20] Nordio, P. L., and Polimeno, A., 1992, *Molec. Phys.*, **75**, 1203.

[21] Polimeno, A., and Nordio, P. L., 1992, *Chem. Phys. Lett.*, **192**, 509.

[22] Van der Zwan, G., and Hynes, G. T., 1970, *J. phys. Chem.*, **89**, 6353.

[23] Moro, G. J., Nordio, P. L., and Polimeno, A., 1989, *Molec. Phys.*, **68**, 1131.

[24] Segre, U., 1983, *Molec. Crystals liq. Crystals*, **90**, 239.

[25] Luckhurst, G. R., and Zannoni, C., 1975, *Proc. R. Soc.* A, **343**, 389.

[26] Nordio, P. L., Rigatti, G., and Segre, U., 1973, *Molec. Phys.*, **25**, 129.

[27] Moro, G., and Freed, J. H., 1986, *Large Scale Eigenvalue Problems*, edited by J. Cullum and R. A. Willoughby (North-Holland), p. 143.

[28] Polimeno, A., and Freed, J. H., 1992, *Adv. Chem. Phys.*, **83**, 89.

[29] Williams, G., 1993, *The Molecular Dynamics of Liquid Crystals*, edited by G. R. Luckhurst and C. Veracini (Kluwer). Chap. 16 (in the press).

[30] Picken, S. J., Gunsteren, W. F., Van Duijnen, P.Th., and de Jeu, W. H., 1989, *Liq. Crystals*, **6**, 357.

[31] Lounila, J., and Diehl, P., 1991, *J. chem. Phys.*, **94**, 1785.

[32] Freed, J. H., Nayeem, A., and Rananavare, S. B., 1993, *The Molecular Dynamics of Liquid Crystals*, edited by G. R. Luckhurst and C. Veracini (Kluwer), Chap. 4 (in the press).

[33] Weiss, R. G., 1988, *Tetrahedron*, **44,** 3413.

[34] Naciri, J., Spada, G. P., Gottarelli, G., and Weiss, R. G., 1987, *J. Am. chem. Soc.*, **109,** 4352.

[35] Brochard, F., and de Gennes, P. G., 1970, *J. Phys., Paris*, **31,** 47.

[36] Brink, D. M., and Satchler, G. R., 1975, *Angular Momentum* (Clarendon).

[37] van Kampen, N. G., 1981, *Stochastic Processes in Physics and Chemistry* (North-Holland), Chap. XI.

[38] Moro, G., and Nordio, P. L., 1985, *Molec. Phys.*, **56,** 255; 1986, *Ibid.*, **57,** 947.

[39] Kramers, H. A., 1940, *Physica*, **7,** 284.

[40] Baraldi, I., Ponterini, G., and Momicchioli, F., 1987, *J. chem. Soc. Faraday Trans.* II, **83,** 2139.

[41] Tsuzuki, S., Tanabe, K., Nagawa, Y., and Nakanishi, H., 1990, *J. molec. Structure*, **216,** 279.

[42] Barbara, P. F., and Jarzeba, W., 1990, *Adv. Photochem.*, **15,** 1.

[43] Pansu, R. B., and Yoshihara, K., 1991, *J. phys. Chem.*, **95,** 10123.

[44] Kang, T. J., Jarzeba, W., Barbara, P. F., and Fonseca, T., 1990, *Chem. Phys.*, **149,** 81.

[45] Moro, G., and Nordio, P. L., 1985, *J. phys. Chem.*, **89,** 997.